nature medicine

Single phosphorylation sites in Acc1 and Acc2 regulate lipid homeostasis and the insulin-sensitizing effects of metformin

Morgan D Fullerton[1,2,9], Sandra Galic[3,9], Katarina Marcinko[1,2], Sarah Sikkema[1,2], Thomas Pulinilkunnil[4], Zhi-Ping Chen[3], Hayley M O'Neill[1–3,5], Rebecca J Ford[1,2], Rengasamy Palanivel[1,2], Matthew O'Brien[3,5], D Grahame Hardie[6], S Lance Macaulay[7], Jonathan D Schertzer[1,2,8], Jason R B Dyck[4], Bryce J van Denderen[3], Bruce E Kemp[3,5] & Gregory R Steinberg[1–3]

The obesity epidemic has led to an increased incidence of nonalcoholic fatty liver disease (NAFLD) and type 2 diabetes. AMP-activated protein kinase (Ampk) regulates energy homeostasis and is activated by cellular stress, hormones and the widely prescribed type 2 diabetes drug metformin[1,2]. Ampk phosphorylates mouse acetyl-CoA carboxylase 1 (Acc1; refs. 3,4) at Ser79 and Acc2 at Ser212, inhibiting the conversion of acetyl-CoA to malonyl-CoA. The latter metabolite is a precursor in fatty acid synthesis[5] and an allosteric inhibitor of fatty acid transport into mitochondria for oxidation[6]. To test the physiological impact of these phosphorylation events, we generated mice with alanine knock-in mutations in both Acc1 (at Ser79) and Acc2 (at Ser212) (Acc double knock-in, AccDKI). Compared to wild-type mice, these mice have elevated lipogenesis and lower fatty acid oxidation, which contribute to the progression of insulin resistance, glucose intolerance and NAFLD, but not obesity. Notably, AccDKI mice made obese by high-fat feeding are refractory to the lipid-lowering and insulin-sensitizing effects of metformin. These findings establish that inhibitory phosphorylation of Acc by Ampk is essential for the control of lipid metabolism and, in the setting of obesity, for metformin-induced improvements in insulin action.

Genetic disruption of Acc1 (refs. 7,8) or Acc2 (refs. 9–12) has yielded conflicting results as to the role of these enzymes in controlling fatty acid metabolism. The Ampk-mediated phosphorylation of Acc1 at Ser79 (Acc1 Ser79, equivalent to Acc2 Ser212) inhibits catalytic activity in cell-free systems[13]. To test the importance of Ampk signaling to Acc *in vivo*, we generated Acc1-S79A and Acc2-S212A knock-in mice and intercrossed these strains to generate AccDKI mice (**Supplementary Fig. 1a**,**b**). We examined Ampk-mediated phosphorylation of liver Acc1 Ser79 and Acc2 Ser212 by mass spectrometry and confirmed the absence of phosphorylation at these sites in the AccDKI but not the wild-type (WT) mice (**Fig. 1a** and **Supplementary Fig. 1c**). We observed no change in baseline Ampk Thr172 phosphorylation in livers from all three lines and no change in the expression of either Acc isoform (**Fig. 1a**). The activities of Acc1 and Acc2 were elevated in AccDKI mice (**Fig. 1b**,**c**) compared to WT controls, consistent with Ampk phosphorylation negatively regulating Acc1 and Acc2 enzyme activity *in vivo*. Furthermore, dephosphorylation of liver Acc1 using lambda phosphatase increased enzyme activity in liver from WT but not AccDKI mice (**Supplementary Fig. 2a**), indicating that Ser79 is the main regulatory site for Acc1 activity. Both WT and AccDKI enzymes remained sensitive to citrate activation, confirming that other mechanisms of Acc regulation remained intact in the AccDKI livers.

Liver malonyl-CoA content is dependent on Acc activity for synthesis and on malonyl-CoA decarboxylase activity for degradation. AccDKI mice had elevated liver malonyl-CoA in the fed state compared to WT control mice (**Fig. 1d**), but this did not result in compensatory upregulation of malonyl-CoA decarboxylase transcript level (**Supplementary Fig. 2b**). Hepatocytes from AccDKI mice had higher *de novo* lipogenesis (**Fig. 1e**) and lower fatty acid oxidation (**Fig. 1f**) compared to those from WT controls. Consistent with this, AccDKI mice also had higher hepatic *de novo* lipogenesis *in vivo* (**Supplementary Fig. 2c**) than WT mice. In contrast, single mutations in Acc1 or Acc2 had minimal changes in these parameters, indicating redundancy between Acc isoforms (**Supplementary Fig. 2d–f**), which is consistent with a previous siRNA knockdown study[14].

[1]Department of Medicine, Division of Endocrinology and Metabolism, McMaster University, Hamilton, Ontario, Canada. [2]Department of Biochemistry and Biomedical Sciences, McMaster University, Hamilton, Ontario, Canada. [3]St. Vincent's Institute of Medical Research, Fitzroy, Victoria, Australia. [4]Cardiovascular Research Centre, Mazankowski Alberta Heart Institute, Department of Pediatrics, Faculty of Medicine and Dentistry, University of Alberta, Edmonton, Alberta, Canada. [5]Department of Medicine, University of Melbourne, Fitzroy, Victoria, Australia. [6]Division of Cell Signaling and Immunology, College of Life Sciences, University of Dundee, Dundee, Scotland, UK. [7]Commonwealth Scientific and Industrial Research Organisation Preventative Health Flagship, Materials Science and Engineering, Parkville, Victoria, Australia. [8]Department of Pediatrics, McMaster University, Hamilton, Ontario, Canada. [9]These authors contributed equally to this work. Correspondence should be addressed to G.R.S. (gsteinberg@mcmaster.ca).

Received 20 February; accepted 11 September; published online 3 November 2013; doi:10.1038/nm.3372

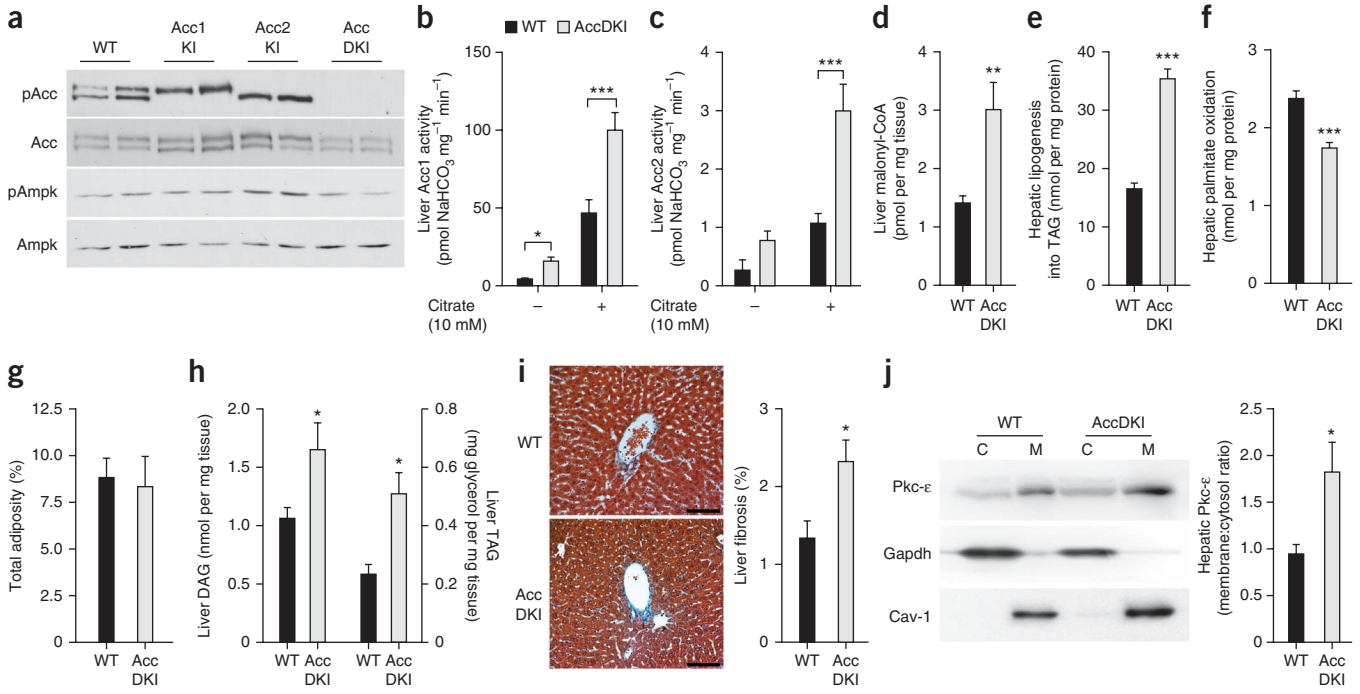

Figure 1 Acc1 Ser79 and Acc2 Ser212 are essential for inhibiting enzyme activity and regulating liver fatty acid metabolism. (**a**) Representative western blot of Ampk-α Thr172, Acc1 Ser79 (bottom band) and Acc2 Ser212 (top band) phosphorylation in liver of WT, Acc1KI, Acc2KI and AccDKI mice. pAcc, phosphorylated Acc. (**b**,**c**) Acc1 (**b**) and Acc2 (**c**) activity with and without citrate (10 mM) in WT and AccDKI liver ($n = 5$ WT and $n = 6$ AccDKI). (**d**) Liver malonyl-CoA abundance in the fed state ($n = 8$). (**e**,**f**) The incorporation of [^{3}H]acetate into TAG as a measure of *de novo* lipogenesis (**e**) and [^{14}C]palmitate oxidation (**f**) in primary hepatocytes ($n = 3$, from at least three separate experiments). (**g**) Total adiposity in chow-fed WT and AccDKI mice ($n = 10$ WT and $n = 14$ AccDKI). (**h**) Liver DAG and TAG ($n = 6$ WT and $n = 8$ AccDKI). (**i**) Histological representation (left) and quantification (right) of collagen staining in liver sections ($n = 6$). Scale bars, 100 μm. (**j**) Activation of liver Pkc-ε as demonstrated by membrane association ($n = 7$). Data are expressed as means ± s.e.m. $^*P < 0.05$, $^{**}P < 0.01$ and $^{***}P < 0.001$ relative to WT, as determined by analysis of variance (ANOVA) and Bonferonni *post hoc* test or Student's *t*-test. For Pkc activation, Gapdh and caveolin-1 (Cav-1) were used for cytosolic (C) and membrane (M) normalization, respectively, and blots shown are from duplicate gels.

Skeletal muscle is the major tissue contributing to the basal metabolic rate, and Acc2 and malonyl-CoA have been shown to be important in regulating skeletal muscle fatty acid oxidation in some[9,11] but not all[10,12] studies. We found that relative to WT controls, malonyl-CoA was higher in skeletal muscle of AccDKI mice (**Supplementary Fig. 2g**), whereas fatty acid oxidation was slightly lower (**Supplementary Fig. 2h**). These data indicate that liver and skeletal muscle malonyl-CoA content and fatty acid metabolism are sensitive to the regulatory phosphorylation of Acc1 at Ser79 and Acc2 at Ser212.

We examined the phenotype of AccDKI mice fed a standard chow diet. Growth curves (data not shown) and adiposity were similar (**Fig. 1g**), but liver (**Fig. 1h**) and skeletal muscle (**Supplementary Fig. 2i**) diacylglycerol (DAG) and triacylglycerol (TAG) levels were elevated in AccDKI compared to WT mice. There were no differences in ceramide content in either tissue (data not shown). Elevated hepatic lipid content in AccDKI mice was associated with clinical signs of NAFLD, including an increased level of fibrosis (**Fig. 1i**) and a slightly elevated serum ratio of alanine aminotransferase to aspartate aminotransferase (**Supplementary Fig. 2j**) compared to WT controls. Pathological accumulation of DAG has been shown to activate atypical isoforms of protein kinase C (Pkc)[15], specifically Pkc-ε and Pkc-δ in liver[16] and Pkc-θ in skeletal muscle[17], which have been shown to interfere with canonical insulin signaling. Consistent with this, AccDKI mice had greater amounts of membrane-associated (**Fig. 1j**) and phosphorylated Pkc-ε (**Supplementary Fig. 3a**) in liver and Pkc-θ in skeletal muscle (**Supplementary Fig. 3b**) compared to control animals, whereas amounts of membrane-associated Pkc-δ did not differ between AccDKI and WT mice (data not shown). These results demonstrate that Acc Ser79 and Ser212 phosphorylation play an essential part in preventing ectopic lipid accumulation independent of body mass or adiposity.

The storage of excess lipid in insulin-sensitive organs such as liver and skeletal muscle is strongly associated with insulin resistance[15,18]. We found that AccDKI mice were hyperglycemic (**Fig. 2a**), hyperinsulinemic (**Fig. 2b**) and also glucose (**Fig. 2c**) and insulin intolerant (**Fig. 2d**) compared to WT controls. Hyperinsulinemic-euglycemic clamp experiments (**Supplementary Fig. 3c**) revealed that AccDKI mice had a lower glucose infusion rate (GIR) (**Fig. 2e**), a lower glucose disposal rate (GDR) (**Fig. 2e**), elevated hepatic glucose production (HGP) (**Fig. 2f**) and a lower suppression of HGP by insulin (**Fig. 2g**) compared to WT controls. Further, livers from AccDKI mice had reduced Akt kinase (Ser473) and FoxO1 transcription factor (Ser253) phosphorylation (**Fig. 2h**,**i**) and higher gluconeogenic gene expression at the completion of the clamp (**Fig. 2j**) compared to WT controls. In addition, we found that c-Jun N-terminal kinase (Jnk), which also inhibits canonical insulin signaling[19], was unchanged in livers from chow-fed AccDKI mice (**Supplementary Fig. 3d**). We observed a trend toward decreased 2-deoxyglucose (2-DG) uptake into skeletal muscle of AccDKI mice during the clamp (**Supplementary Fig. 3e**) and a marked reduction in muscle Akt (Ser473) and FoxO1 (Ser253) phosphorylation (**Supplementary Fig. 3f**,**g**) at the completion of the

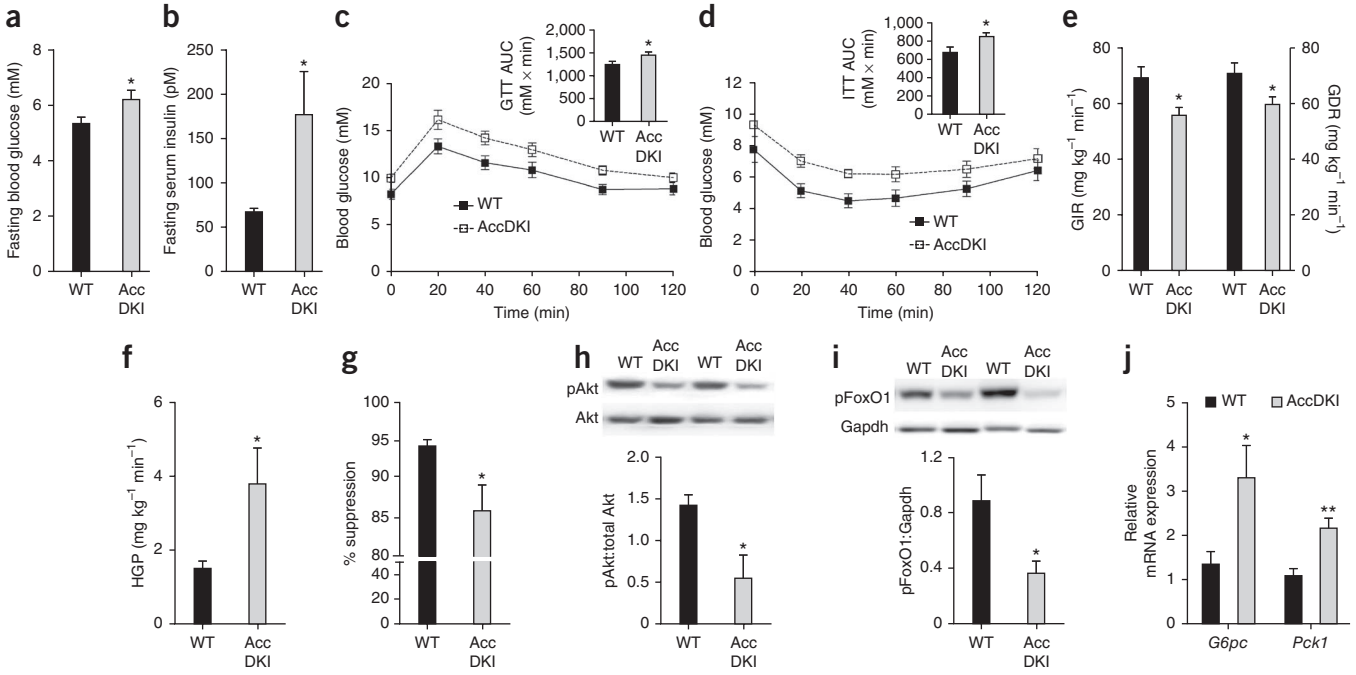

Figure 2 AccDKI mice fed a control diet are glucose intolerant and have hepatic insulin resistance. (**a**–**d**) Fasting blood glucose (**a**), fasting serum insulin levels (**b**), glucose tolerance test (GTT) (2 g per kg body weight) (**c**) and insulin tolerance test (ITT) (0.6 U per kg body weight) (**d**) ($n = 10$ WT and $n = 14$ AccDKI) in WT and AccDKI mice. AUC, area under the curve. (**e**–**g**) Hyperinsulinemic-euglycemic clamp results: GIR and GDR (**e**), HGP (**f**) and suppression of hepatic glucose production (**g**) ($n = 7$ WT and $n = 8$ AccDKI). (**h**–**j**) Liver Akt (Ser473) phosphorylation (**h**), liver FoxO1 (Ser253) phosphorylation (**i**) and gluconeogenic gene expression (*G6pc* and *Pck1*) (**j**) in the liver at the completion of the clamp ($n = 7$ WT and $n = 8$ AccDKI). Data are expressed as means ± s.e.m. $^*P < 0.05$ and $^{**}P < 0.01$ relative to WT, as determined by Student's *t*-test. Relative gene expression was normalized to *Actb*, and duplicate gels were run for quantification of total Akt and Gapdh.

clamp compared to WT control mice. Furthermore, insulin resistance in AccDKI mice was independent of changes in liver or adipose tissue macrophage accumulation, inflammatory cytokine gene expression or protein content (**Supplementary Fig. 4a**–**c**) or differences in circulating free fatty acids (**Supplementary Fig. 4d**). These results indicate that Acc phosphorylation is required to maintain insulin sensitivity in lean healthy mice. Notably, mice with complete deletions of Ampk isoforms in skeletal muscle[20] or liver[21] have normal lipid levels and insulin sensitivity, suggesting that in these models, there may be alterations in compensatory pathways that are important for controlling fatty acid metabolism.

Over 120 million people are prescribed metformin for the management of type 2 diabetes[22]. As metformin indirectly activates Ampk, it was initially thought that Ampk mediates metformin's therapeutic actions[23]. However, acute inhibition of gluconeogenesis by metformin is independent of Ampk[21] and involves inhibition of glucagon signaling through protein kinase A (Pka)[24]. Nevertheless, the ability of metformin to lower blood glucose in obese individuals with type 2 diabetes involves chronic enhancement in insulin sensitivity[25–29]. We found that acute metformin treatment activated hepatic Ampk in both genotypes, but this was only associated with increased Acc phosphorylation (**Fig. 3a**) and reduced malonyl-CoA levels (**Fig. 3b**) in WT mice. Metformin reduced *de novo* lipogenesis in hepatocytes from WT mice, and this suppressive effect was equivalent to that caused by Ampk-β1–specific activation using A-769662 (ref. 30) (**Fig. 3c**). Notably, the metformin-induced inhibition of hepatic lipogenesis seen upon Ampk activation was entirely mediated by Ampk phosphorylation of Acc, as metformin and A-769662 were ineffective at suppressing lipogenesis in AccDKI or Ampk-β1–deficient hepatocytes (**Fig. 3c**). However, unlike A-769662, metformin did not increase fatty acid oxidation in either genotype (**Supplementary Fig. 4e**). These data demonstrate that the effects of metformin on lipogenesis are specific to Ampk and indicate that although Ampk may inhibit multiple targets in this pathway, including sterol regulatory element binding protein-1c (ref. 31) and expression of fatty acid synthase[32], the primary regulation of lipogenesis is dependent on the phosphorylation of both Acc1 and Acc2. In contrast, lipogenesis was inhibited by metformin in hepatocytes from both WT and Acc1 knock-in (Acc1KI) mice (**Supplementary Fig. 4f**), and *in vivo*, a lipid-lowering effect was demonstrated in high-fat diet (HFD)-fed WT and Acc1KI animals treated with metformin (**Supplementary Fig. 4g**).

In humans, therapeutic doses of metformin (0.5–3 g per day)[27] result in plasma concentrations ranging from 10 to 25 μM (refs. 33,34). In rodents, the administration of 50 mg per kg body weight of metformin has been shown to elicit plasma concentrations of 29 μM (ref. 35). We therefore treated HFD-fed WT and AccDKI mice with a daily dose of metformin at 50 mg per kg body weight for 6 weeks. In contrast to chow-fed mice, HFD-fed AccDKI mice showed no differences in any metabolic parameters compared to HFD-fed WT animals (**Fig. 3** and **Supplementary Figs. 5**–**7**). This indicates that diet-induced obesity overwhelms the effect of signaling by endogenous Ampk to Acc unless an external Ampk stimulus is provided.

Metformin has been shown to have positive effects on fatty liver in some but not all clinical trials[25]. However, rodent studies with metformin have demonstrated a clear lipid-lowering effect[23,30], which suggests the need for more robust analyses or the development of more reliable biomarkers in human studies[25,36]. Notably, *in vivo*

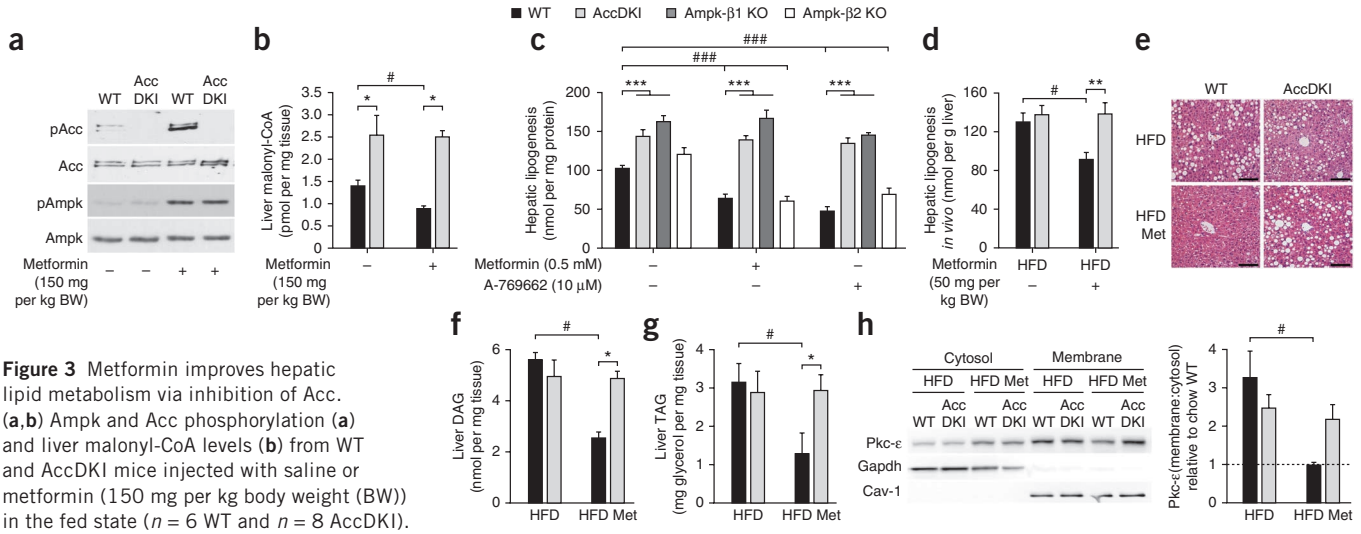

Figure 3 Metformin improves hepatic lipid metabolism via inhibition of Acc. (**a**,**b**) Ampk and Acc phosphorylation (**a**) and liver malonyl-CoA levels (**b**) from WT and AccDKI mice injected with saline or metformin (150 mg per kg body weight (BW)) in the fed state ($n = 6$ WT and $n = 8$ AccDKI). (**c**) Incorporation of [^{3}H]acetate into the total lipid fraction (*de novo* lipogenesis) in primary hepatocytes ($n = 3$ from at least three separate experiments). KO, knockout. (**d**) *In vivo* incorporation of [^{3}H]acetate into total liver lipid (*de novo* lipogenesis) in HFD-fed WT and AccDKI mice treated with vehicle or metformin (50 mg per kg body weight) ($n = 11$ for vehicle and $n = 6$ for metformin). (**e**–**g**) Representative staining (H&E) of hepatic sections (**e**) (scale bars, 100 μm) and determination of hepatic DAG (**f**) and TAG (**g**) ($n = 7$ WT and $n = 8$ AccDKI) from WT and AccDKI mice fed a HFD for 12 weeks, with or without concurrent metformin (Met) (50 mg per kg body weight per day) starting after 6 weeks of HFD (HFD Met). (**h**) Activation of hepatic Pkc-ε, shown as the ratio of membrane to cytosolic expression and expressed relative to chow WT control ($n = 7$) (cytosol normalized to Gapdh and membrane normalized to caveolin-1 (Cav-1); blots shown are from duplicate gels). Data are expressed as means ± s.e.m. $^*P < 0.05$, $^{**}P < 0.01$ and $^{***}P < 0.001$ compared to WT control and $^{\#}P < 0.05$ and $^{\#\#\#}P < 0.01$ are differences between treatment, as calculated by two-way ANOVA and Bonferonni *post hoc* test.

lipogenesis was similar between HFD-fed WT and AccDKI mice (**Fig. 3d**), and an acute dose of metformin (50 mg per kg body weight) suppressed lipogenesis *in vivo* by ~35% in WT livers yet was completely ineffective in AccDKI mice (**Fig. 3d**). We next assessed the metabolic effects of chronic metformin treatment and found that, independent of change in weight or adiposity (**Supplementary Fig. 5c**), hepatic lipid content was reduced in WT mice, an effect completely absent in AccDKI mice (**Fig. 3e**–**g**). Reductions in hepatic DAG were accompanied by decreased membrane-associated (**Fig. 3h**) and Ser729-phosphorylated Pkc-ε (**Supplementary Fig. 5d**) and lower Jnk activation (**Supplementary Fig. 5e**) in metformin-treated WT but not AccDKI mice.

In addition to reducing hepatic lipid content, chronic metformin treatment of HFD-fed WT but not AccDKI mice was associated with lowered fasting blood glucose (**Fig. 4a**), a trend toward lowered serum insulin levels (**Supplementary Fig. 5f**) and improved glucose tolerance (**Supplementary Fig. 5g**) and insulin sensitivity (**Fig. 4b**). Metformin-induced suppression of cAMP and glucagon-dependent hepatic glucose output is independent of Ampk[21,24], and in hepatocytes from WT, AccDKI and Ampk-β1–deficient mice, metformin was effective at suppressing cAMP-stimulated glucose production (**Supplementary Fig. 5h**). Metformin was also able to acutely lower circulating glucose levels in both chow-fed and obese HFD-fed WT and AccDKI mice, as shown by metformin tolerance tests (200 mg per kg body weight[37]) (**Supplementary Fig. 5i**). However, at the dose that was used for our chronic treatments (50 mg per kg body weight), glucose levels were unaltered (**Supplementary Fig. 5j**), strongly suggesting that metabolic differences following chronic metformin treatment between AccDKI and WT mice were primarily the result of differential regulation of insulin sensitivity rather than acute effects on glucose lowering.

In hyperinsulinemic-euglycemic clamp experiments, chronic metformin treatment improved GDR (**Supplementary Fig. 6a**) and skeletal muscle 2-DG uptake in both WT and AccDKI mice (**Supplementary Fig. 6b**,**c**). This is consistent with an Ampk-Pkc–dependent pathway controlling metformin-induced skeletal muscle glucose uptake[38]. In contrast, chronic metformin treatment increased GIR (**Supplementary Fig. 6d**–**g**), decreased HGP (**Fig. 4c**) and increased suppression of HGP by insulin (**Fig. 4d**) in WT but not AccDKI mice. Enhanced Akt (Ser473) and FoxO1 (Ser253) phosphorylation (**Supplementary Fig. 7a**,**b**) and reduced gluconeogenic gene expression (**Supplementary Fig. 7c**) at the completion of the clamp in WT but not in AccDKI mice provides further evidence of metformin-induced improvements in hepatic insulin sensitivity. We demonstrated that metformin improved insulin sensitivity in a liver cell-autonomous manner in a cellular model of palmitate-induced insulin resistance. In particular, hepatocytes made insulin resistant by chronic treatment (18 h) with the saturated fatty acid palmitate were treated with metformin, which improved insulin-stimulated phosphorylation of Akt Ser473 and FoxO1 Ser253 (**Fig. 4e**), insulin-induced suppression of gluconeogenic gene expression (**Fig. 4f**) and insulin-induced suppression of hepatic glucose production (**Fig. 4g**) in hepatocytes from WT but not AccDKI mice. Notably, the beneficial metabolic effects of specific Ampk activation by A-769662 were completely abrogated in AccDKI hepatocytes and *in vivo* (**Supplementary Fig. 8a**–**d**), which corroborates the fundamental importance of Ampk-Acc signaling for hepatic lipid metabolism and insulin sensitivity.

Metformin remains the primary therapeutic option for the treatment of type 2 diabetes, although the precise mechanisms by which it confers its beneficial effects are incompletely understood. Glucagon-driven hepatic gluconeogenesis maintains glycemia during states of fasting, and this is poorly regulated in patients with type 2 diabetes. Recently, it has been shown that metformin counters this program by inhibiting glucagon-stimulated cAMP production, thereby reducing Pka activity and glucagon-stimulated glucose output from

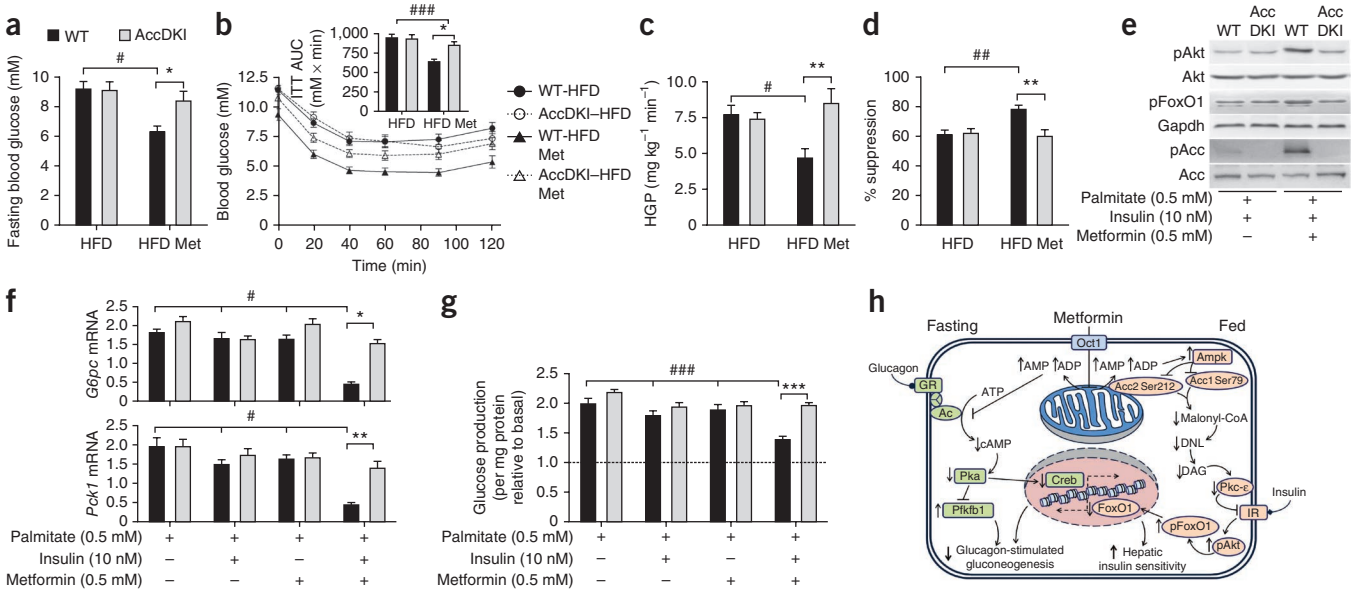

Figure 4 HFD-fed AccDKI mice are insensitive to metformin-induced improvements in liver insulin sensitivity. (**a**–**d**) WT and AccDKI mice fed a HFD for 6 weeks were given daily metformin (50 mg per kg body weight) for an additional 6 weeks (HFD Met). Fasting blood glucose (**a**) and insulin tolerance test (1 U per kg body weight) (**b**) ($n = 10$ HFD-fed WT and AccDKI; $n = 12$ WT and $n = 16$ AccDKI–HFD Met). The effect of metformin treatment on HGP (**c**) and suppression of HGP by insulin (**d**) ($n = 7$ WT and $n = 9$ AccDKI). (**e**,**f**) Akt (Ser473) and FoxO1 (Ser253) phosphorylation (**e**) and *G6pc* and *Pck1* expression (**f**) in isolated hepatocytes treated with chronic palmitate (18 h) and stimulated with insulin, where gene expression is shown relative to the WT condition without palmitate. (**g**) Hepatic glucose production, following chronic (18 h) exposure to palmitate (0.5 mM) in the presence or absence of metformin (0.5 mM), then in response to Bt_2-cAMP (100 μM) and insulin (10 nM) for 4 h, in the absence of acute metformin. ($n = 3$, from at least three separate experiments). Hatched line represents control hepatocytes not stimulated with Bt_2-cAMP for glucose production. (**h**) Schematic representation of metformin's therapeutic effects on hepatic action during differential nutrient and hormonal programs. Oct1, organic cation transporter 1; GR, glucagon receptor; Ac, adenylate cyclase; DNL, *de novo* lipogenesis; Creb, cAMP response element–binding protein; Pfkfb1, 6-phosphofructo-2-kinase/fructose-2,6-bisphosphatase 1; IR, insulin receptor. Data are expressed as means ± s.e.m. $^{*}P < 0.05$, $^{**}P < 0.01$ and $^{***}P < 0.001$ represent differences between genotype and $^{\#}P < 0.05$, $^{\#\#}P < 0.01$ and $^{\#\#\#}P < 0.001$ are differences between treatment, as calculated by two-way ANOVA and Bonferonni *post hoc* test.

the liver[24]. We confirmed that this mechanism also operates in both WT and AccDKI mice in response to high concentrations of metformin (**Supplementary Fig. 8e**). An important distinction between this previous work[24] and our current study is their focus on the fasting, or glucagon-specific, actions of metformin, which occur in the absence of insulin stimulation. The ability of insulin to suppress hepatic gluconeogenesis and to promote the efficient uptake of glucose in the periphery is fundamental and dramatically decreased in insulin resistance and type 2 diabetes.

The insulin-sensitizing effects of metformin have been well documented[25,28,29], but mechanistic insight has been lacking. Our data provide evidence that in the setting of obesity and insulin resistance, chronic metformin treatment (at a clinical dose) reduces hepatic lipogenesis and lipid accumulation by activation of Ampk and consequent inhibition of both Acc1 and Acc2. This lipid-lowering effect then alleviates obesity-induced insulin resistance. Notwithstanding metformin inhibition of glucagon-dependent gluconeogenesis, we provide evidence for a parallel mechanism, whereby chronic metformin treatment increases insulin sensitivity through alterations in hepatic lipid homeostasis (**Fig. 4h**).

Since the initial discovery that Ampk directly phosphorylates Acc1, the site-specific phosphorylation of Acc1 and Acc2 has been used as a surrogate marker for Ampk signaling in hundreds of studies. Currently, more than 30 other substrates of Ampk have been identified in multiple metabolic pathways. Through genetic targeting of Acc1 Ser79 and Acc2 Ser212 and the generation of knock-in mice, we show that phosphorylation and inhibition of these two Ampk substrates is critical for maintaining lipid metabolism and insulin sensitivity. Moreover, Acc phosphorylation by Ampk also underpins the insulin-sensitizing effects of metformin.

METHODS

Methods and any associated references are available in the online version of the paper.

Note: Any Supplementary Information and Source Data files are available in the online version of the paper.

ACKNOWLEDGMENTS

We thank C. Saab from the McMaster Centre for Translational Imaging for completing the computed tomography analysis and S. Stypa and E. Day for technical assistance. This study was supported by grants and fellowships from the Australian Research Council and the Commonwealth Scientific and Industrial Research Organisation (B.E.K.), the Australian National Health and Medical Research Council (B.E.K., B.J.v.D. and G.R.S.), the Canadian Diabetes Association (G.R.S., J.R.B.D. and J.D.S.) and the Canadian Institutes of Health Research (CIHR) (G.R.S. and J.R.B.D.) and was supported in part by the Victorian Government Operational Infrastructure Support Program (B.E.K.) and the Canadian Foundation for Innovation (G.R.S.). M.D.F. is supported by a CIHR Banting Postdoctoral Fellowship, J.D.S. is supported by a Canadian Diabetes Association Scholar Award and G.R.S. holds a Canada Research Chair in Metabolism and Obesity.

AUTHOR CONTRIBUTIONS

M.D.F., S.G., B.E.K. and G.R.S. designed the study. M.D.F., S.G., K.M., S.S., R.J.F. and R.P. performed *in vivo* experiments. M.D.F., S.G. and J.D.S. performed primary hepatocyte experiments. S.G., Z.-P.C. performed Acc activity assays and M.O. performed mass spectrometry experiments. H.M.O. performed fatty acid oxidation in isolated skeletal muscle. T.P. and J.R.B.D. measured tissue malonyl-CoA content. D.G.H. contributed Acc antibodies for activity assays and helpful comments

regarding the manuscript. B.J.v.D., S.L.M., B.E.K. and G.R.S. were involved in generating the knock-in mice. M.D.F. and G.R.S. wrote the manuscript.

COMPETING FINANCIAL INTERESTS

The authors declare no competing financial interests.

1. Kahn, B.B., Alquier, T., Carling, D. & Hardie, D.G. AMP-activated protein kinase: ancient energy gauge provides clues to modern understanding of metabolism. *Cell Metab.* **1**, 15–25 (2005).
2. Long, Y.C. & Zierath, J.R. AMP-activated protein kinase signaling in metabolic regulation. *J. Clin. Invest.* **116**, 1776–1783 (2006).
3. Carlson, C.A. & Kim, K.H. Regulation of hepatic acetyl coenzyme A carboxylase by phosphorylation and dephosphorylation. *J. Biol. Chem.* **248**, 378–380 (1973).
4. Carling, D., Zammit, V.A. & Hardie, D.G. A common bicyclic protein kinase cascade inactivates the regulatory enzymes of fatty acid and cholesterol biosynthesis. *FEBS Lett.* **223**, 217–222 (1987).
5. Wakil, S.J., Stoops, J.K. & Joshi, V.C. Fatty acid synthesis and its regulation. *Annu. Rev. Biochem.* **52**, 537–579 (1983).
6. McGarry, J.D., Leatherman, G.F. & Foster, D.W. Carnitine palmitoyltransferase I. The site of inhibition of hepatic fatty acid oxidation by malonyl-CoA. *J. Biol. Chem.* **253**, 4128–4136 (1978).
7. Harada, N. *et al.* Hepatic *de novo* lipogenesis is present in liver-specific ACC1-deficient mice. *Mol. Cell Biol.* **27**, 1881–1888 (2007).
8. Mao, J. *et al.* Liver-specific deletion of acetyl-CoA carboxylase 1 reduces hepatic triglyceride accumulation without affecting glucose homeostasis. *Proc. Natl. Acad. Sci. USA* **103**, 8552–8557 (2006).
9. Abu-Elheiga, L., Matzuk, M.M., Abo-Hashema, K.A. & Wakil, S.J. Continuous fatty acid oxidation and reduced fat storage in mice lacking acetyl-CoA carboxylase 2. *Science* **291**, 2613–2616 (2001).
10. Hoehn, K.L. *et al.* Acute or chronic upregulation of mitochondrial fatty acid oxidation has no net effect on whole-body energy expenditure or adiposity. *Cell Metab.* **11**, 70–76 (2010).
11. Olson, D.P., Pulinilkunnil, T., Cline, G.W., Shulman, G.I. & Lowell, B.B. Gene knockout of Acc2 has little effect on body weight, fat mass, or food intake. *Proc. Natl. Acad. Sci. USA* **107**, 7598–7603 (2010).
12. Choi, C.S. *et al.* Continuous fat oxidation in acetyl-CoA carboxylase 2 knockout mice increases total energy expenditure, reduces fat mass, and improves insulin sensitivity. *Proc. Natl. Acad. Sci. USA* **104**, 16480–16485 (2007).
13. Munday, M.R., Campbell, D.G., Carling, D. & Hardie, D.G. Identification by amino acid sequencing of three major regulatory phosphorylation sites on rat acetyl-CoA carboxylase. *Eur. J. Biochem.* **175**, 331–338 (1988).
14. Savage, D.B. *et al.* Reversal of diet-induced hepatic steatosis and hepatic insulin resistance by antisense oligonucleotide inhibitors of acetyl-CoA carboxylases 1 and 2. *J. Clin. Invest.* **116**, 817–824 (2006).
15. Erion, D.M. & Shulman, G.I. Diacylglycerol-mediated insulin resistance. *Nat. Med.* **16**, 400–402 (2010).
16. Samuel, V.T. *et al.* Inhibition of protein kinase Cepsilon prevents hepatic insulin resistance in nonalcoholic fatty liver disease. *J. Clin. Invest.* **117**, 739–745 (2007).
17. Yu, C. *et al.* Mechanism by which fatty acids inhibit insulin activation of insulin receptor substrate-1 (IRS-1)-associated phosphatidylinositol 3-kinase activity in muscle. *J. Biol. Chem.* **277**, 50230–50236 (2002).
18. Chibalin, A.V. *et al.* Downregulation of diacylglycerol kinase δ contributes to hyperglycemia-induced insulin resistance. *Cell* **132**, 375–386 (2008).
19. Hirosumi, J. *et al.* A central role for JNK in obesity and insulin resistance. *Nature* **420**, 333–336 (2002).
20. O'Neill, H.M. *et al.* AMP-activated protein kinase (AMPK) β1β2 muscle null mice reveal an essential role for AMPK in maintaining mitochondrial content and glucose uptake during exercise. *Proc. Natl. Acad. Sci. USA* **108**, 16092–16097 (2011).
21. Foretz, M. *et al.* Metformin inhibits hepatic gluconeogenesis in mice independently of the LKB1/AMPK pathway via a decrease in hepatic energy state. *J. Clin. Invest.* **120**, 2355–2369 (2010).
22. Viollet, B. *et al.* Cellular and molecular mechanisms of metformin: an overview. *Clin. Sci. (Lond.)* **122**, 253–270 (2012).
23. Zhou, G. *et al.* Role of AMP-activated protein kinase in mechanism of metformin action. *J. Clin. Invest.* **108**, 1167–1174 (2001).
24. Miller, R.A. *et al.* Biguanides suppress hepatic glucagon signalling by decreasing production of cyclic AMP. *Nature* **494**, 256–260 (2013).
25. Musso, G., Cassader, M., Rosina, F. & Gambino, R. Impact of current treatments on liver disease, glucose metabolism and cardiovascular risk in non-alcoholic fatty liver disease (NAFLD): a systematic review and meta-analysis of randomised trials. *Diabetologia* **55**, 885–904 (2012).
26. Bailey, C.J. & Mynett, K.J. Insulin requirement for the antihyperglycaemic effect of metformin. *Br. J. Pharmacol.* **111**, 793–796 (1994).
27. Bailey, C.J. & Turner, R.C. Metformin. *N. Engl. J. Med.* **334**, 574–579 (1996).
28. Gómez-Sámano, M.Á. *et al.* Metformin and improvement of the hepatic insulin resistance index independent of anthropometric changes. *Endocr. Pract.* **18**, 8–16 (2012).
29. Natali, A. & Ferrannini, E. Effects of metformin and thiazolidinediones on suppression of hepatic glucose production and stimulation of glucose uptake in type 2 diabetes: a systematic review. *Diabetologia* **49**, 434–441 (2006).
30. Cool, B. *et al.* Identification and characterization of a small molecule AMPK activator that treats key components of type 2 diabetes and the metabolic syndrome. *Cell Metab.* **3**, 403–416 (2006).
31. Li, Y. *et al.* AMPK phosphorylates and inhibits SREBP activity to attenuate hepatic steatosis and atherosclerosis in diet-induced insulin-resistant mice. *Cell Metab.* **13**, 376–388 (2011).
32. Foretz, M., Carling, D., Guichard, C., Ferre, P. & Foufelle, F. AMP-activated protein kinase inhibits the glucose-activated expression of fatty acid synthase gene in rat hepatocytes. *J. Biol. Chem.* **273**, 14767–14771 (1998).
33. Lalau, J.D., Lemaire-Hurtel, A.S. & Lacroix, C. Establishment of a database of metformin plasma concentrations and erythrocyte levels in normal and emergency situations. *Clin. Drug Investig.* **31**, 435–438 (2011).
34. Owen, M.R., Doran, E. & Halestrap, A.P. Evidence that metformin exerts its anti-diabetic effects through inhibition of complex 1 of the mitochondrial respiratory chain. *Biochem. J.* **348**, 607–614 (2000).
35. Wilcock, C. & Bailey, C.J. Accumulation of metformin by tissues of the normal and diabetic mouse. *Xenobiotica* **24**, 49–57 (1994).
36. Clark, J.M., Brancati, F.L. & Diehl, A.M. Nonalcoholic fatty liver disease. *Gastroenterology* **122**, 1649–1657 (2002).
37. He, L. *et al.* Metformin and insulin suppress hepatic gluconeogenesis through phosphorylation of CREB binding protein. *Cell* **137**, 635–646 (2009).
38. Turban, S. *et al.* Defining the contribution of AMP-activated protein kinase (AMPK) and protein kinase C (PKC) in regulation of glucose uptake by metformin in skeletal muscle cells. *J. Biol. Chem.* **287**, 20088–20099 (2012).

ONLINE METHODS

Animals. Both Acc1-S79A KI and Acc2-S212A KI mice were generated by OzGene Pty (Perth, Australia). The targeting strategy is summarized in **Supplementary Figure 1**. The generation of Ampk-β1–deficient and Ampk-β2–deficient mice has previously been described[39,40]. All mice used in the study were bred on a C57BL/6 background and from heterozygous intercrosses. Male mice were used for all studies and housed in specific-pathogen–free microisolators and maintained on a 12-h light-dark cycle with lights on at 7:00 a.m. Mice were maintained on either a chow diet (17% kcal from fat; Diet 8640, Harlan Teklad, Madison, WI) or HFD (45% kcal from fat; D12451, Research Diets; New Brunswick, NJ) starting at 6 weeks of age for 12 weeks. For HFD-metformin experiments, mice received 6 weeks of daily intraperitoneal injections of metformin (50 mg per kg body weight) starting after 6 weeks of the HFD. Fasting and fed blood samples were collected for serum analyses through submandibular bleeding. The McMaster University (Hamilton, Canada) Animal Ethics Research Board and St. Vincent's Hospital (Melbourne, Australia) Animal Ethics Committee approved all experimental protocols.

Enzymatic activity assays. Acc activity in liver was measured by $^{14}CO_2$ fixation into acid-stable products. Acc1 or Acc2 protein was immunoprecipitated from 2 mg of tissue homogenates using Acc1- or Acc2-specific antibodies. Acc1- and Acc2-specific antibodies were generated by immunizing sheep with synthetic peptides coupled to keyhole limpet hemocyanin (CDEPSPLAKTLELNQ (rat Acc1 (1–15 Cys^1) and CEDKKQAPIKRQLMT (rat Acc2 (145–159 Cys^{145})) and purifying antibodies from the resulting sera by affinity chromatography on immobilized peptides. Immunoprecipitates were incubated for 1.5 h at room temperature with reaction buffer containing 125 μM acetyl-CoA, 12.5 mM $NaHCO_3$ and 16.7 μCi/ml [^{14}C]$NaHCO_3$ with the indicated concentrations of citrate. The reactions were terminated by addition of HCl and dried overnight at 37 °C. Water was added to the dried sample and radioactivity measured by liquid scintillation counting. Purified Acc1 proteins from WT and Acc1KI livers were subjected to λ phosphatase (400 U in a 60-μl reaction) treatment for 25 min at 30 °C. After a wash removal of the phosphatase, a small aliquot was used for determination of Acc1 Ser79 phosphorylation by western blot analysis. The majority of the protein that remained was used to assess Acc activity, as described above.

Mass spectrometry analyses. Acc isoforms from WT and AccDKI livers were affinity-purified by streptavidin. Proteins were eluted from beads, reduced and alkylated with iodoacetamide and then precipitated with methanol/chloroform (1:1, vol/vol). The denatured proteins were digested overnight with trypsin in solution at 37 °C. Peptides were separated on a PepMap RSLC C_{18} column using a Dionex 3000 Series NCS-3500RS nano liquid chromatography system. Mass spectrometry was performed on a 5600 Triple TOF MS (AB SCIEX).

Malonyl-CoA assay. Quantification of short-chain CoA species was performed as reported previously with modification[41]. Briefly, frozen muscle and liver samples (~15–20 mg) were homogenized for 20 s in 300 μl of 6% (vol/vol) perchloric acid. After homogenization, the samples were left on ice for 10 min and then centrifuged at 12,000*g* for 5 min. The resulting supernatant (100 μl) was analyzed using a UPLC Waters Acquity System. Each sample was run at a flow rate of 0.4 ml/min through an Ascentis Express C_{18} Column, 10 cm × 2.1 mm and 2.7-μm particle size from Supelco maintained at a temperature of 40 °C. The analyte detection occurred at an absorbance of 260 nm. The mobile phase consisted of a mixture of buffer A (0.25 M NaH_2PO_4 and water) and buffer B (0.25 M NaH_2PO_4 and acetonitrile). The gradient-elution profile consisted of the following initial conditions: 2% B for 2–4 min, 25% B for 4–6 min, 40% B for 6–8 min and 100% B for 10–12 min, maintained for 15 min. All gradients were linear and peaks were acquired, integrated and analyzed using the Waters Empower Software.

Histological analyses. Tissues were fixed in formalin for at least 48 h, embedded in paraffin and H&E stained. After staining, each sample was imaged in triplicate. For determination of hepatic fibrosis, trichrome staining was used to visualize collagen. This was then quantified using the color segmentation function of Image J software (National Institutes of Health).

Western blotting, inflammation and RT-PCR. Tissues were dissected rapidly, snap-frozen in liquid nitrogen and stored at −80 °C until subsequent analyses. All primary antibodies were used at a dilution of 1:1,000. Blotting for total and phosphorylated Akt, Jnk, Ampk and Acc (antibodies all from Cell Signaling: Akt #9272, pAkt Ser473 #4058, Jnk #9252, pJNK #9251, AMPK-α #2532, pAMPK-α Thr172 #2531, Acc #3676, pAcc Ser79 #3661 and β-actin #5125) were performed as previously described[42]. Phosphorylated FoxO1 Ser253 (Cell Signaling #9461) was normalized to Gapdh (Cell Signaling #2118). For Pkc-ε phosphorylation, an antibody directed against Ser729 was used (Abcam ab134031). For membrane-associated Pkc activation, tissues were homogenized in 300 μl of buffer I (20 mM Tris·HCl, pH 7.4, 1 mM EDTA, 0.25 mM EGTA, 250 mM sucrose and protease inhibitor mixture) and centrifuged at 100,000 × *g* for 1 h (4 °C). The supernatants containing the cytosolic fraction were removed to new tubes. Pellets were then resuspended in 300 μl of buffer II (250 mM Tris·HCl, pH 7.4, 1 mM EDTA, 0.25 mM EGTA, 2% Triton X-100 and protease inhibitor mixture) and centrifuged at 100,000 × *g* for 1 h (4 °C) to obtain the plasma membrane fraction. Gapdh and caveolin-1 were used as markers of the cytosolic and membrane preparation purity, respectively. Pkc-ε, Pkc-θ and Pkc-δ activation (Cell signaling Pkc- ε #2683, Pkc-θ #2059 and Pkc-δ #2058) was expressed as a ratio of membrane (normalized to caveolin-1(BD Biosciences #C37120)) to cytosolic (normalized to Gapdh) localization, which was assessed from the same membrane to eliminate exposure bias. Hepatic tissues were prepared as previously described[43], and proinflammatory cytokines were determined using commercially available kits. Total RNA isolation, cDNA synthesis and quantitative RT-PCR were performed as described previously[42].

Metabolic studies. For glucose, insulin and metformin tolerance tests, mice were injected with D-glucose (2 g per kg body weight and 1 g per kg body weight for chow and HFD, respectively), human insulin (0.6 U per kg body weight and 1 U per kg body weight for chow and HFD, respectively) or 50 and 200 mg per kg body weight metformin[37] through intraperitoneal injection and blood glucose monitored at the indicated times by a small cut in the tail vein. Whole-body adiposity was assessed by computed tomography, and respiratory exchange ratio was determined using Columbus Laboratory Animal Monitoring System as previously described[42]. Hyperinsulinemic-euglycemic clamps were performed as previously described[42]. Briefly, 5 d after cannulation, only mice that lost <8% of their weight were clamped. Mice fasted 6 h were infused with a basal infusate containing D-[3-^{3}H]glucose (7.5 μCi/h, 0.12 ml/h) for 1 h to determine basal glucose disposal. An insulin infusate (10 mU insulin per kg body weight per min in 0.9% saline) containing D-[3-^{3}H]glucose (7.5 μCi/h, 0.12 ml/h) was then initiated and blood glucose monitored and titrated with 50% dextrose infused at a variable rate to achieve and maintain euglycemia. For rates of glucose uptake, [^{14}C]2-DG (10 μCi) was infused during the clamped state and tissues excised after 30 min. The rates of glucose disposal in the basal and clamped states and hepatic glucose output were calculated using the Steele equation for steady-state conditions[44]. Insulin was measured by ELISA kit, alanine aminotransferase and aspartate aminotransferase were determined using commercially available kits and TAG levels were determined by glycerol assay following saponification of the TAG fraction separated using thin-layer chromatography. Total levels of tissue DAG and ceramides were quantified using DAG kinase assay as previously described[45]. *de novo* lipogenesis was determined *in vivo* by the incorporation of [^{3}H]acetate into hepatic lipids after metformin (50 mg per kg body weight) or A-769662 (30 mg per kg body weight) injection, where saline and 5% DMSO in PBS served as vehicles, respectively. Skeletal muscle fatty acid oxidation was assessed in isolated extensor digitorum longus muscle as previously described[40]. For metformin-stimulated glucose uptake, isolated extensor digitorum longus muscle was incubated with vehicle (60 min), metformin (1 mM for 60 min), submaximal insulin (2.0 μM for 30 min) or metformin (1 mM for 60 min) plus insulin (2.0 μM for 30 min). 2-DG uptake was then measured over 20 min in the presence of insulin (2 μM) or metformin (1 mM). To measure hepatic cAMP, WT and AccDKI mice in the fed condition were

injected with vehicle, 200 or 400 mg per kg body weight metformin. After 1 h, mice received a vehicle or glucagon injection (2 mg per kg body weight). Livers were collected after 5 min and rapidly freeze-clamped[23]. Hepatic cAMP measurements were performed using an EIA from Cayman Chemicals per the manufactures instructions.

Cell culture experiments. Primary hepatocytes were isolated by collagenase perfusion[42]. [^{3}H]acetate lipogenesis and [^{14}C]palmitate oxidation was performed as described previously[39]. Briefly, for lipogenesis, [^{3}H]acetate (5 μCi/ml) was in the presence of 0.5 mM sodium acetate for 4 h. Medium was then removed and cells washed with PBS before lipid extraction for determination of incorporation into lipid fractions. For fatty acid oxidation, [^{14}C]palmitate (2 μCi/ml) was in the presence of 0.5 mM palmitate (conjugated to 2% BSA) for 4 h. Medium was removed and acidified with equal volume of 1 M acetic acid in an airtight vial. [^{14}C]CO_2 was trapped in 400 μl of 1 M benzethonium hydroxide and radioactivity determined. Cellular lipids were extracted after a PBS wash, and radioactivity of the acid soluble intermediates was determined. Total oxidation was then calculated as a function of both [^{14}C]CO_2–produced and incomplete oxidation products. For insulin signaling experiments in hepatocytes, cells were incubated in the presence or absence of 0.5 mM palmitate (conjugated to 2% BSA) and 0.5 mM metformin for 18 h (with 0.1% FBS). Cells were then stimulated with 10 nM insulin; gluconeogenic gene expression was assessed after 6 h of insulin treatment, and insulin signaling was assessed after 5 min of insulin stimulation. Hepatic glucose production was determined as previously described[22]. Briefly, cells were cultured as above in the presence of 100 nM dexamethasone. Cells were washed once with PBS and incubated in glucose-free DMEM (100 nM dexamethasone, 10 mM lactate and 1 mM pyruvate) with or without Bt_2-cAMP (100 μM) and with or without indicated doses of metformin or A-769662. For chronic treatments, palmitate-, metformin- and A-769662–supplemented medium was removed after 18 h, cells were washed and glucose-free DMEM was added to measure glucose output in the presence or absence of insulin (10 nM). Glucose in the medium after 4 h was assessed by glucose oxidase kit.

Statistical analyses. All results shown are mean ± s.e.m. Results were analyzed using a two-tailed Student's *t*-test or two-way ANOVA, where appropriate, using GraphPad Prism software. A Bonferonni *post hoc* test was used to test for significant differences revealed by the ANOVA. Significance was accepted at $P \leq 0.05$.

39. Dzamko, N. *et al.* AMPK β1 deletion reduces appetite, preventing obesity and hepatic insulin resistance. *J. Biol. Chem.* **285**, 115–122 (2010).
40. Steinberg, G.R. *et al.* Whole body deletion of AMP-activated protein kinase β2 reduces muscle AMPK activity and exercise capacity. *J. Biol. Chem.* **285**, 37198–37209 (2010).
41. Ussher, J.R. *et al.* Stimulation of glucose oxidation protects against acute myocardial infarction and reperfusion injury. *Cardiovasc. Res.* **94**, 359–369 (2012).
42. Galic, S. *et al.* Hematopoietic AMPK β1 reduces mouse adipose tissue macrophage inflammation and insulin resistance in obesity. *J. Clin. Invest.* **121**, 4903–4915 (2011).
43. Schertzer, J.D. *et al.* NOD1 activators link innate immunity to insulin resistance. *Diabetes* **60**, 2206–2215 (2011).
44. Steele, R. Influences of glucose loading and of injected insulin on hepatic glucose output. *Ann. NY Acad. Sci.* **82**, 420–430 (1959).
45. Preiss, J. *et al.* Quantitative measurement of *sn*-1,2-diacylglycerols present in platelets, hepatocytes, and *ras*- and *sis*-transformed normal rat kidney cells. *J. Biol. Chem.* **261**, 8597–8600 (1986).

doi:10.1038/nm.3372